# Transverse expansion of the electron sheath during laser acceleration of protons

K. Svensson,[1] F. Mackenroth,[2,3] L. Senje,[1] A. Gonoskov,[3] C. Harvey,[3] B. Aurand,[1,a)]
M. Hansson,[1] A. Higginson,[4] M. Dalui,[1] O. Lundh,[1] P. McKenna,[4] A. Persson,[1]
M. Marklund,[3] and C.-G. Wahlström[1,b)]
[1]*Department of Physics, Lund University, 221 00 Lund, Sweden*
[2]*Max Planck Institute for the Physics of Complex Systems, Nöthnitzer Str. 38, 01187 Dresden, Germany*
[3]*Chalmers University of Technology, 412 58 Gothenburg, Sweden*
[4]*SUPA Department of Physics, University of Strathclyde, Glasgow G4 0NG, United Kingdom*

(Received 23 October 2017; accepted 21 November 2017; published online 12 December 2017)

The transverse expansion of the electrostatic sheath during target normal sheath acceleration of protons is investigated experimentally using a setup with two synchronized laser pulses. With the pulses spatially separated by less than three laser spot diameters, the resulting proton beam profiles become elliptical. By introducing a small intensity difference between the two pulses, the ellipses are rotated by a certain angle, except if the spatial separation of the two laser pulses is in the plane of incidence. The rotation angle is shown to depend on the relative intensity of the two pulses. The observed effects are found to require high temporal contrasts of the laser pulses. A simple model describing how the transverse shape of the electron sheath on the rear of the target depends on the relative intensity between the foci is presented. The model assumptions are verified, and the unknown dependence of the transverse extents of the sheaths are estimated self-consistently through a series of high resolution, two-dimensional particle-in-cell simulations. The results predicted by the model are also shown to be consistent with those obtained from the experiment.

https://doi.org/10.1063/1.5010173

## I. INTRODUCTION

The study of compact sources of the laser-driven energetic proton beams is an active area of research, with many potential applications, such as proton oncology,[1] production of short-lived isotopes,[2] and ion implantation.[3] One acceleration process, called target-normal sheath acceleration (TNSA), has emerged as a robust acceleration mechanism over a range of parameters.[4,5] The process incorporates a short laser pulse, typically shorter than 1 ps, which carries an energy of 1–100 J. The laser pulse is focused onto the front surface of a thin foil, which is instantly ionized and becomes a plasma that starts to expand. The resulting plasma electron density, $n_e$, has a gradient along the target normal direction, and at a certain plane, parallel to the target surface, becomes higher than the critical density, $n_c = \varepsilon_0 m_e \omega^2 / e^2$, for the laser radiation, where $\varepsilon_0$ is the permittivity of free space, $m_e$ is the electron mass, $\omega$ is the laser angular frequency, and $e$ is the elementary charge. This has the effect that the laser pulse cannot propagate through the full length of the plasma and is partially reflected. However, some of its energy is absorbed and heats the electrons, which can traverse the target. There are different heating mechanisms contributing to the hot electron population, such as resonant absorption,[6] vacuum heating,[7] and $J \times B$ heating.[8] For high intensities and short plasma scale lengths, $J \times B$ heating is expected to dominate, which predominantly accelerates hot electrons along the laser propagation axis. As the electrons exit the rear of the target, they set up strong electrostatic sheath fields, which ionize atoms and molecules present on the rear surface of the target, and accelerate the resulting positively charged particles. Earlier studies have shown that it is possible to manipulate the beam profile of the accelerated protons by either altering the target geometry[9,10] or by controlling the laser intensity distribution on the front of the target.[11]

In a recent study,[12] we showed that, by varying the laser intensity distribution on the front of the target, the divergence of the resulting proton beam can be controlled. Irradiating the target simultaneously at an oblique incidence with two identical, focused laser pulses, spatially separated by less than three spot diameters, resulted in an accelerated proton beam with an elliptical transverse profile, with its major axis perpendicular to the foci separation axis. However, separating the foci by more than three spot diameters resulted in two independent proton sources on the rear of the target, and the proton beam profiles observed some centimeters away from the target were circular, just as if only one focus was used. In this paper, we extend that study and present new experimental results, partly expounded in the theses by Svensson[13] and Senje,[14] obtained by altering the intensity ratio between the two separated laser foci. We find that under certain conditions the orientation of the ellipse rotates, which enables us to determine how the transverse expansion of the electron sheath field depends on laser pulse intensity.

a)Present address: Institut für Laser- and Plasmaphysik, Heinrich-Heine Universität, 40225 Düsseldorf, Germany
b)Electronic mail: claes-goran.wahlstrom@fysik.lth.se

 

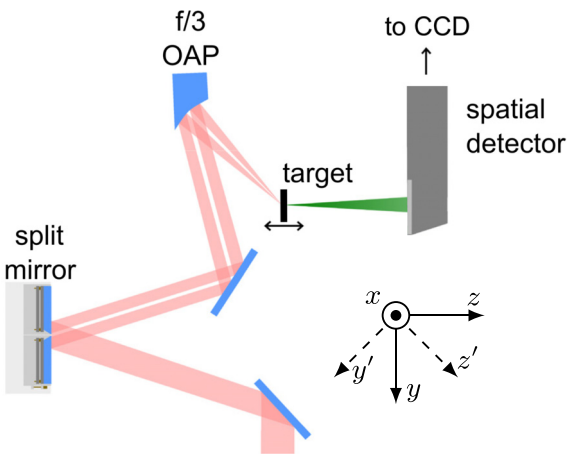


FIG. 1. A p-polarized laser pulse is guided onto the split mirror, where it is divided in two parts. Both of them are directed towards an f/3 off-axis parabolic mirror, which focuses the laser pulses onto the front of a 3 $\mu$m thick aluminum target foil. The accelerated protons are detected by a spatially resolving detector, situated 6.5 cm from the rear of the target. The illustration is adapted from Aurand *et al.*,[12] in which the experimental setup is described in greater detail.

## II. EXPERIMENTAL SETUP

The experimental investigation was performed using the multi-terawatt laser system at the Lund Laser Centre, which for this study delivered p-polarized laser pulses with full-width at half-maximum (FWHM) durations of 40 fs, and temporal contrasts higher than $10^9$ on the 100 ps time scale. The central wavelengths of the laser pulses were 0.8 $\mu$m. The total energy on target for each laser pulse was 0.7 J. The experimental setup[15] is illustrated in Fig. 1. A split mirror divides the incoming laser pulse into two separate pulses, and both are focused by the same f/3 off-axis parabolic mirror (OAP) onto the front of a 3 $\mu$m-thick aluminum foil at 45° incidence angle, resulting in two spots, each with a size (intensity FWHM) of 5 $\mu$m. By introducing a controlled tilt in one part of the split mirror, it is possible to separate the two foci horizontally and/or vertically. Their relative intensity can also be varied by moving the split mirror relative to the laser beam. During the experimental study, the accelerated protons were detected by a spatially resolving detector situated 6.5 cm from the rear of the target. The spatially resolving detector is essentially a scintillating screen (Saint-Gobain, BC-408), which is imaged onto one end of an optical fiber bundle. The other end is, in turn, imaged by a 12 bit camera, positioned outside the experimental vacuum chamber. The scintillator is covered by a 13 $\mu$m thick aluminum foil in order to protect it from residual laser light and target debris. This foil also stops protons with energies lower than ∼1 MeV and heavy ions.

## III. RESULTS AND DISCUSSION

### A. Experimental results

When the two vertically separated laser pulses had equal intensity, as in Fig. 2(b), the resulting spatial profile of the proton beam was elliptical with its major axis oriented horizontally [see Fig. 2(f)]. This is in agreement with the findings by Aurand *et al.*[12] Introducing a small intensity difference between the two laser pulses, the elliptical proton beam profile became tilted by an angle $\alpha$, as shown in Figs. 2(a) and 2(e). If the rotation angle of the elliptical beam profile depends on differences in laser spot characteristics between the two foci, inverting their positions should mirror the proton beam profile about the horizontal axis. This was experimentally verified, and the orientation of the elliptical proton beam profile was indeed reversed when the two foci were changed as shown in Figs. 2(c) and 2(g). For horizontal separation of the laser foci, the elliptical proton beam profile was oriented vertically. However, introducing an intensity difference in this configuration did not result in any significant rotation of the ellipse from its vertical orientation.

To determine how $\alpha$ is affected by the relative foci alignment, we positioned the separated laser foci, with equal intensities, at an angle $\varphi$ relative to the vertical axis. By keeping the separation distance fixed and varying $\varphi$ from 0° to 90°, we found that the resulting $\alpha$ followed $\varphi$ in a one-to-one relation. Thus, the observed effect, shown in Fig. 2, is significantly larger than can be accounted for by any misalignments of the laser foci, estimated to be less than ±5°. However, for horizontal separation of the foci, any tilt was well within the alignment precision regardless of the intensity ratio.

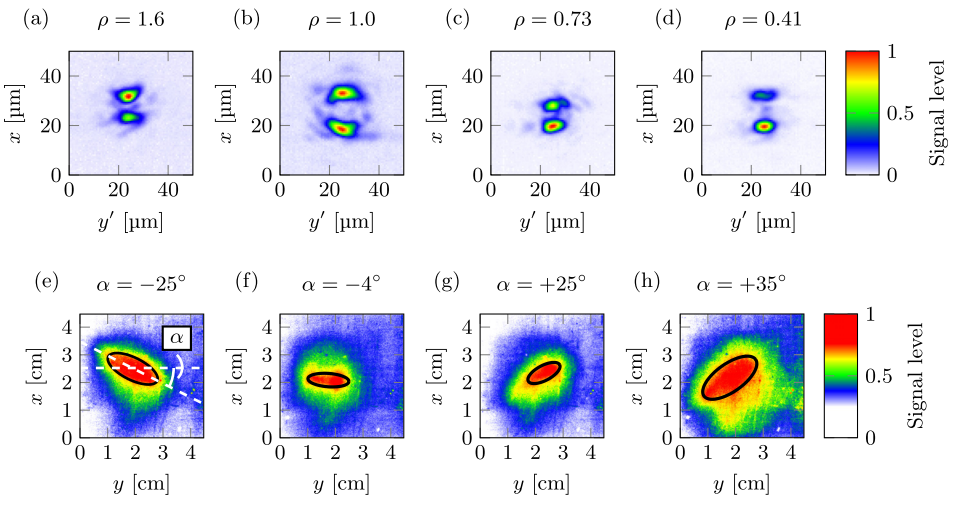


FIG. 2. Vertically separated laser foci with (a) $\rho = 1.6$, (b) $\rho = 1.0$, (c) $\rho = 0.73$, and (d) $\rho = 0.41$, where $\rho$ is the intensity ratio from the peak values in each image. The corresponding transverse proton beam profiles are depicted in (e)–(h). In (a) and (c), the foci are separated 8.5 $\mu$m, and in (b) and (d) by 12 $\mu$m. The proton beam profile rotation angles, $\alpha$, are approximately (e) –25°, (f) –4°, (g) +25°, and (h) +35°. The ellipses are fitted to the 60% signal level, and all color scales are normalized to the maximum signal in each image. Each proton beam profile is recorded 6.5 cm from the target foil.

The observations can be explained if the transverse shape of the electrostatic sheath field, responsible for proton acceleration, is tilted. Since the angle of incidence of the laser is 45° in the horizontal plane, the sheath expansion on the target rear surface is expected to have a preferred direction along the positive $y$-axis (as defined in Fig. 1). Also, if $J \times B$ heating dominates, the lateral expansion of the sheath will preferentially be in that direction, since the electrons are driven in the laser propagation ($z'$) direction (see Fig. 1). Thus, separating the foci vertically (along the $x$-axis), and introducing a difference in expansion through an intensity difference, the leading edge of the resulting electron sheath becomes tilted. Separating the foci horizontally (along the $y'$-axis), on the other hand, does not result in any tilt of the transverse front of the electrostatic sheath field.

### B. Theoretical model and simulations

To describe the effect quantitatively, we construct a simple model describing the transverse sheath expansion. We start from the basic assumption that for each laser focus $S_1$ and $S_2$, the spatial size of the resulting sheath field depends on the laser energies contained in each focus. We neglect any changes in laser spot sizes and assume the pulse duration to remain unaffected by the splitting of the laser pulse. Then, separating the foci by a distance $d$, their different transverse front edge positions $y_1$ and $y_2$, respectively, lead to an effective tilting of the transverse shape of the leading edge of the sheath by an angle $\theta$, as indicated in Fig. 3. Since the major axis of the elliptical proton beam profile for equal intensity in the two foci, was found to be perpendicular to the orientation of the elongated sheath field,[12] we assume here that $\alpha = -\theta$. From geometrical considerations, we find from Fig. 3,

$$\tan(\theta) = \frac{y_1 - y_2}{d}. \tag{1}$$

Assuming the edge position scaling with laser pulse intensity to be equivalent and independent in the two laser spots, it is sufficient to consider here only one spot, in order to analytically derive the dependency of $\theta$ on the ratio, $\rho = I_1/I_2$, between the peak intensity in respective foci, and the total laser energy $E_{\text{tot}}$.

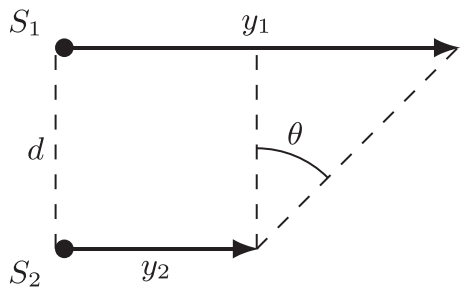


FIG. 3. A model where the two laser spots, $S_1$ and $S_2$, are separated vertically by a distance $d$. Each laser spot creates a sheath, which extends along the positive $y$-axis (see Fig. 1 for axis definitions) by $y_1$ and $y_2$, respectively. The figure illustrates the situation after a given expansion time, when the intensity of the laser pulse in $S_1$ was higher than in $S_2$.

We model the edge position of the sheath arising from a single laser spot to depend linearly on the laser pulse energy in that spot. Below, we confirm this assumption to be well reproduced by numerical simulations in the parameter range under study. Then, the energy-dependent edge position on the rear side of the target is parametrized as

$$y(E) = kE + \mathcal{C}, \tag{2}$$

where $k$ and $\mathcal{C}$ are constants. Inserting Eq. (2) into Eq. (1), we find $\theta$ to be given by

$$\tan(\theta) = \frac{k}{d} E_{\text{tot}} \frac{\rho - 1}{\rho + 1}. \tag{3}$$

The only unknown parameter in Eq. (3) is the proportionality constant $k$. To determine it, we invoke numerical simulations. Since we are only interested in the sheath dynamics in the plane of incidence of the laser pulse ($yz$-plane), a two-dimensional cut through the laser spot is expected to provide a good model of the expanding sheath. We perform a series of two-dimensional particle-in-cell (PIC) simulations, using the code PICADOR.[16] We simulate a linearly polarized laser pulse with central wavelength $\lambda = 0.81$ $\mu$m and a Gaussian envelope in time with 66 fs FWHM pulse duration and a focal spot diameter 5 $\mu$m incident under a 45° angle onto a 3 $\mu$m thick, preionized target. On the front of the target, we simulate a preplasma of scale length $L = 0.1$ $\mu$m, composed of electrons (mass $m_e$, charge $-e$) and protons (mass $m_p$, charge $e$). The target bulk is composed of electrons and highly ionized heavy ions (mass to charge ratio $4.5m_p/e$). We check that higher ionization states in the target bulk, as are expected to occur in the experiment (i.e., lower mass to charge ratios in the simulations) do not significantly alter the simulation results. We use a simulation box with $4096 \times 1024$ cells and a size of 160 $\mu$m $\times$ 60 $\mu$m to resolve the small scale plasma heating dynamics as well as the large spatial extent of the sheath expansion. We initialize the simulation such that at its start, the center of the laser pulse is 15 $\mu$m from the front of the target, to suppress artificial penetration of the main laser pulse into the target.

All parameters are kept unchanged in the series of simulations, except for the energy content of the laser pulse, which is varied in the range 0.025 J to 1.5 J. Then, for each separate simulation the proton density on the rear side of the target is recorded as a function of time, with an example displayed in Fig. 4. Clearly visible is a structure with significantly reduced proton density growing over time. We interpret this lack of protons being due to the expanding electron cloud accelerating them away from the rear side of the target. The sheath field is subsequently screened by the accelerated protons whence no protons are pulled back into the sheath region over the times studied here, and a proton void signifies the spatial extent of the sheath on the rear side of the target. We then use an automated routine to fit a smeared out step profile of the form $n_p(y) = n_{p0}(1 - \exp[-\sigma_{n_p} y^4])$ to the proton distribution in the positive as well as the negative $y$-direction. Here, $n_p$ is the proton density on the rear side of the target, and $n_{p0}$ and $\sigma_{n_p}$ are fitting

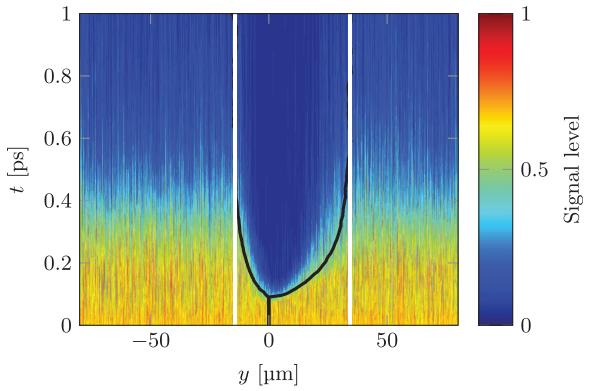


FIG. 4. Example of PIC simulation results for a single laser pulse with energy 1.1 J, showing the proton density as a function of both $y$, and time, $t$. The transverse edge position of the sheath is extracted from the region void of protons, and the fitted edge position for each time step is shown as black lines, with the saturated size shown as white lines.

parameters. For each time step in the simulation, we identify the edge position as the position $y_{\text{sheath}}$ where the fitted step profile has reached $n_p(y_{\text{sheath}}) = 0.9n_{p0}$ (black lines in Fig. 4). Apparently, the edge position saturates to a constant value ∼0.5 ps after the laser pulse has passed. This is interpreted as the equilibrium edge position in the positive as well as the negative $y$-direction (white lines in Fig. 4). We note that by using the positive edge position in Eq. (1) as the location of the main contribution to the accelerating field, we implicitly assume the ion acceleration to be dominated by the leading edge of the expanding sheath. This assumption is motivated by the observation from the simulations that upon the impact of the laser pulse, a surface wave is formed at the leading edges of the sheath on the rear side of the target. This surface wave provides the main accelerating field responsible for the acceleration of protons.

The resulting energy dependent sheath edge position in the positive $y$-direction is shown in Fig. 5 and is described well by a line for laser energies $E > 0.1$ J. Therefore, we limit the use of the presented linear model to laser energies higher than this threshold. In this regime, we find Eq. (2) to provide a good reproduction of the energy dependent edge position, with the proportionality constant determined to be

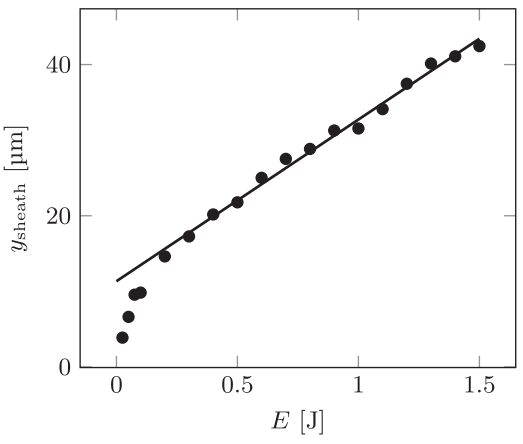


FIG. 5. Fitted edge positions in the forward direction for the performed PIC simulations. The solid line is a linear fit for $E > 0.1$ J, with slope $k = 21\ \mu\text{m J}^{-1}$.

$k = 21\ \mu\text{m J}^{-1}$. Thus, with a given $\rho$, $E_{\text{tot}}$, and $d$, we can predict the angle of rotation ($\theta$) of the resulting proton beam profile.

### C. Discussion and conclusions

Finally, we compare the predictions of our model to our experimental measurement in Fig. 6 for $E_{\text{tot}} = 0.7$ J, and $\rho$ ranging between 0.41 and 1.6. The experimentally measured rotation angles are shown as black dots, and are in good agreement with our simple model. This indicates that the assumptions underlying the phenomenological model, such as, e.g., the accelerating field being sensitive to the leading transverse edge position of the sheath, reasonably captures the sheath dynamics.

It is also worth noting that $\theta$ is very sensitive to changes in the energy ratio close to $\rho = 1$ for higher laser energy. This effect agrees with the experimental observation that the rotation angle is very sensitive to even small differences in energy between the two laser spots. The ellipticity of the beam profiles and their corresponding orientation is also found to be sensitive to the temporal contrast of the laser pulses, as the effect vanished when the temporal contrasts of the laser pulses were decreased. This is assumed to be related to the plasma expansion on the front of the target. If the scale length of the plasma on the front surface is long, the effects of two separated foci are effectively washed out. The model describing the rotation of the elliptical proton beam profiles also assumes a preferred sheath expansion direction. If $J \times B$ heating is the dominating heating mechanism, in combination with a short scale length, the expansion of the electron sheath on the rear of the target will have a preferred direction along the target surface, in, essentially, the direction of laser propagation. The presented model is rather simple. As explicitly mentioned, we neglect the variations of the size and shape of the focused laser pulses irradiating the target

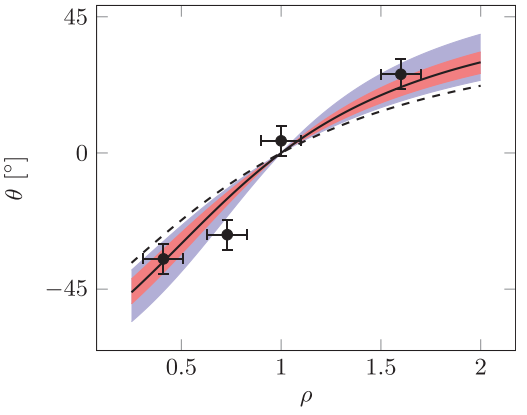


FIG. 6. Rotation angle of the front edge of the electron sheath, $\theta$, as predicted by Eq. (3) as a function of foci energy ratio, $\rho$, is shown for $E_{\text{tot}} = 0.7$ J. The black, solid line corresponds to using $d = 8.5\ \mu$m, and the dashed line corresponds to $d = 12\ \mu$m. The red area surrounding the solid line shows how the $\theta$ changes when $E_{\text{tot}}$ is changed by $\pm 0.1$ J, and the blue area shows how $\theta$ changes when $d$ is changed by $\pm 2.5\ \mu$m. The rotation angles measured experimentally are shown as circles, assuming the relation $\theta = -\alpha$, with error bars indicating estimated uncertainties. The uncertainty of $\theta$ is estimated to $\pm 5°$, and arises from the fact that $\theta$ depends on which signal level is selected for the fitting routine. In $\rho$, the uncertainty is given by using different methods for calculating the energy ratio.

when experimentally altering the energy ratio between the pulses. Furthermore, assuming the tilt of the total sheath field to be due only to the varying steady state transverse edge position in the forward direction disregards more complicated dynamics such as the sheath expansion in the backward direction. Temporal dynamics, due to the fact that the high energy protons are emitted mostly at an early stage of the acceleration, where the forward edge position of the sheath is likely to not yet have reached a steady-state value are also disregarded in our model. In this respect, we note that the satisfying agreement between experiment and theory indicates that our simple model still takes the dominant physics into account. On the other hand, we expect significant improvements of the theoretical model to be possible by, e.g., including more complex dynamics of the acceleration process, or a refined model for the tilt angle of the combined sheath field.

A more detailed study of how $\theta$ varies with $\rho$ and $E_{\mathrm{tot}}$ could be used to benchmark more elaborate models of the transverse sheath expansion. Using the technique introduced in this paper, it would also be possible to measure how the transverse expansion and timescales depend on the incidence angle of the laser pulse.

## ACKNOWLEDGMENTS

We acknowledge the support from the Swedish Research Council, the Knut and Alice Wallenberg Foundation, including their funding of the PLIONA project, and the Swedish Foundation for Strategic Research.

[1]S. V. Bulanov and V. S. Khoroshkov, Plasma Phys. Rep. **28**, 453 (2002).
[2]S. Fritzler, V. Malka, G. Grillon, J.-P. Rousseau, F. Burgy, E. Lefebvre, E. d'Humières, P. McKenna, and K. W. D. Ledingham, Appl. Phys. Lett. **83**, 3039 (2003).
[3]L. Torrisi, S. Gammino, A. M. Mezzasalma, J. Badziak, P. Parys, J. Wolowski, E. Woryna, J. Krása, L. Láska, M. Pfeifer, K. Rohlena, and F. P. Boody, Appl. Surf. Sci. **217**, 319 (2003).
[4]H. Daido, M. Nishiuchi, and A. S. Pirozhkov, Rep. Prog. Phys. **75**, 056401 (2012).
[5]A. Macchi, M. Borghesi, and M. Passoni, Rev. Mod. Phys. **85**, 751 (2013).
[6]J. P. Freidberg, R. W. Mitchell, R. L. Morse, and L. I. Rudsinski, Phys. Rev. Lett. **28**, 795 (1972).
[7]F. Brunel, Phys. Rev. Lett. **59**, 52 (1987).
[8]W. L. Kruer and K. Estabrook, Phys. Fluids **28**, 430 (1985).
[9]M. Schollmeier, K. Harres, F. Nürnberg, A. Blazevic, P. Audebert, E. Brambrink, J. C. Fernandez, K. A. Flippo, D. C. Gautier, M. Geissel, B. M. Hegelich, J. Schreiber, and M. Roth, Phys. Plasmas **15**, 053101 (2008).
[10]L. Giuffrida, K. Svensson, J. Pšikal, M. Dalui, H. Ekerfelt, I. Gallardo-González, O. Lundh, A. Persson, P. Lutoslawski, V. Scuderi, J. Kaufman, T. Wiste, T. Lastovicka, A. Picciotto, A. Bagolini, M. Crivellari, P. Bellutti, G. Milluzzo, G. A. P. Cirrone, J. Magnusson, A. Gonoskov, G. Korn, C.-G. Wahlström, and D. Margarone, Phys. Rev. Accel. Beams **20**, 081301 (2017).
[11]D. C. Carroll, P. McKenna, O. Lundh, F. Lindau, C.-G. Wahlström, S. Bandyopadhyay, D. Pepler, D. Neely, S. Kar, P. T. Simpson, K. Markey, M. Zepf, C. Bellei, R. G. Evans, R. Redaelli, D. Batani, M. H. Xu, and Y. T. Li, Phys. Rev. E **76**, 065401 (2007).
[12]B. Aurand, L. Senje, K. Svensson, M. Hansson, A. Higginson, A. Gonoskov, M. Marklund, A. Persson, O. Lundh, D. Neely, P. McKenna, and C.-G. Wahlström, Phys. Plasmas **23**, 023113 (2016).
[13]K. Svensson, "Experiments on laser-based particle acceleration: Beams of energetic electrons and protons," Ph.D. thesis (Lund University, 2016).
[14]L. Senje, "Detector development, source characterization and novel applications of laser ion acceleration," Ph.D. thesis (Lund University, 2017).
[15]B. Aurand, M. Hansson, L. Senje, K. Svensson, A. Persson, D. Neely, O. Lundh, and C.-G. Wahlström, Laser Part. Beams **1**, 59–64 (2014).
[16]S. Bastrakov, R. Donchenko, A. Gonoskov, E. Efimenko, A. Malyshev, I. Meyerov, and I. Surmin, J. Comput. Sci. **3**, 474 (2012).